Neurobiology of Disease 139 (2020) 104821

Contents lists available at ScienceDirect

Neurobiology of Disease

journal homepage: www.elsevier.com/locate/ynbdi

Pathological remodelling of colonic wall following dopaminergic nigrostriatal neurodegeneration

Carolina Pellegrini[a], Chiara Ippolito[b], Cristina Segnani[b], Amelio Dolfi[b], Mariella Errede[c], Daniela Virgintino[c], Matteo Fornai[d], Luca Antonioli[d], Francesca Garelli[e], Anna Nericcio[e], Rocchina Colucci[e], Silvia Cerri[f], Fabio Blandini[f], Corrado Blandizzi[d], Nunzia Bernardini[b,g,*]

[a] Department of Pharmacy, University of Pisa, Pisa, Italy
[b] Unit of Histology and Medical Embryology, Department of Clinical and Experimental Medicine, University of Pisa, Pisa, Italy
[c] Unit of Human Anatomy and Histology, Department of Basic Medical Sciences, Neurosciences and Sensory Organs, School of Medicine, University of Bari, Bari, Italy
[d] Unit of Pharmacology and Pharmacovigilance, Department of Clinical and Experimental Medicine, University of Pisa, Pisa, Italy
[e] Department of Pharmaceutical and Pharmacological Sciences, University of Padova, Padova, Italy
[f] Laboratory of Functional Neurochemistry, Centre for Research in Neurodegenerative Diseases, "C. Mondino" National Neurological Institute, University of Pavia, Pavia, Italy
[g] Interdepartmental Research Centre "Nutraceuticals and Food for Health", University of Pisa, Pisa, Italy

ARTICLE INFO

Keywords:
Parkinson's disease
6-hydroxydopamine
Rat model
Intestinal dysfunctions
Colon
Morphological remodelling
Collagen deposition
Histochemistry
Immunohistochemistry
Immunofluorescence

ABSTRACT

Background and aim: Patients with Parkinson's disease (PD) are often characterized by functional gastrointestinal disorders. Such disturbances can occur at all stages of PD and precede the typical motor symptoms of the disease by many years. However, the morphological alterations associated with intestinal disturbances in PD are undetermined. This study examined the remodelling of colonic wall in 6-hydroxydopamine (6-OHDA)-induced PD rats.

Methods: 8 weeks after 6-OHDA injection animals were sacrificed. Inflammatory infiltrates, collagen deposition and remodelling of intestinal epithelial barrier and *tunica muscularis* in the colonic wall were assessed by histochemistry, immunohistochemistry, immunofluorescence and western blot analysis.

Results: 6-OHDA rats displayed significant alterations of colonic tissues as compared with controls. Signs of mild inflammation (eosinophil infiltration) and a transmural deposition of collagen fibres were observed. Superficial colonic layers were characterized by severe morphological alterations. In particular, lining epithelial cells displayed a reduced claudin-1 and transmembrane 16A/Anoctamin 1 (TMEM16A/ANO1) expression; goblet cells increased their mucin expression; colonic crypts were characterized by an increase in proliferating epithelial cells; the density of S100-positive glial cells and vimentin-positive fibroblast-like cells was increased as well. Several changes were found in the *tunica muscularis*: downregulation of α-smooth muscle actin/desmin expression and increased proliferation of smooth muscle cells; increased vimentin expression and proliferative phenotype in myenteric ganglia; reduction of interstitial cells of Cajal (ICCs) density.

Conclusions: A pathological remodelling occurs in the colon of 6-OHDA rats. The main changes include: enhanced fibrotic deposition; alterations of the epithelial barrier; activation of mucosal defense; reduction of ICCs. These results indicate that central nigrostriatal denervation is associated with histological changes in the large bowel at mucosal, submucosal and muscular level. These alterations might represent morphological correlates of digestive symptoms in PD.

Abbreviations: **GI**, gastrointestinal; **ICCs**, interstitial cells of Cajal; **6-OHDA**, 6-hydroxydopamine; **PCNA**, proliferating cellular nuclear antigen; **PD**, Parkinson's disease; **PPP**, percentage of positive pixels; **S100**, glial cell marker; **α-SMA**, alpha-smooth muscle actin; **SMC**, smooth muscle cell; **SR/FG**, Sirius red/Fast green; **TMEM16A/ANO1**, transmembrane 16A/Anoctamin 1

* Corresponding author at: Unit of Histology and Medical Embryology, Department of Clinical and Experimental Medicine, University of Pisa, Via Roma 55, 56126 Pisa, Italy.
E-mail address: nunzia.bernardini@med.unipi.it (N. Bernardini).

https://doi.org/10.1016/j.nbd.2020.104821
Received 26 August 2019; Received in revised form 30 January 2020; Accepted 19 February 2020
Available online 21 February 2020

1. Introduction

Patients with Parkinson's disease (PD) often experience gastrointestinal dysfunctions, including dyspepsia and constipation, which impact negatively on their quality of life (Pellegrini et al., 2015; Pellegrini et al., 2016a). The occurrence of enteric immune/inflammatory responses could contribute to the onset of intestinal motor disturbances in PD (Pellegrini et al., 2018). Indeed, recent studies have reported intestinal neurochemical and functional alterations and enteric inflammation both in patients and in PD animal models that could contribute to intestinal dysmotility (Devos et al., 2013; Fornai et al., 2016; Pellegrini et al., 2016b; Rota et al., 2019). In this setting, chronic and unresolved bowel inflammation can alter the intestinal epithelial barrier, and, in turn, compromise intestinal permeability and absorptive/secretory functions (Bischoff et al., 2014). Of interest, recent studies reported that PD patients are characterized by impaired intestinal epithelial barrier and colonic inflammation, thus supporting the contention that enteric inflammation and a related remodelling of mucosal barrier could contribute to intestinal disturbances in PD (Clairembault et al., 2015; Devos et al., 2013; Perez-Pardo et al., 2019) It is also acknowledged that the presence of chronic and recurrent enteric inflammation can promote cellular and molecular events that, in turn, can lead to a remarkable remodelling of gut wall, including fibrosis, which could contribute further to bowel motor dysfunctions (Gordon et al., 2014). Indeed, intestinal fibrosis can occur in several bowel disorders characterized by the presence of chronic inflammation (e.g., inflammatory bowel diseases, drug-induced enteropathy and sigmoid diverticulitis) (Speca et al., 2012). In particular, intestinal fibrosis can lead to a massive collagen deposition and extracellular matrix components, which then promote a deep unsettlement of tissue architecture, followed by functional dysregulation and onset of complications, with negative outcomes for patients' health and quality of life (Rieder et al., 2007).

Whether the intestinal inflammation observed in PD is associated with gut tissue remodelling, with particular regard for intestinal fibrosis and alterations of mucosal barrier, remains still unclear. On these basis, the present study examined morphological and molecular changes in full-thickness colonic wall in a rat model of PD induced by injection of 6-hydroxydopamine (6-OHDA). This knowledge provides new insights to a better understanding of the mechanisms underlying bowel disturbances associated with PD and designing rational therapeutic approaches.

2. Methods

2.1. Induction and evaluation of nigrostriatal denervation

Male Sprague-Dawley rats, 200–250 g body weight, were surgically treated and pharmacologically lesioned to obtain a nigrostriatal denervation as reported previously (Fornai et al., 2016). The experiments were performed in accordance with the provisions of the European Community Council Directive 86–609, recognized and adopted by the Italian Government and approved by the Ethical Committee for Animal Experimentation of the Italian Ministry of Health.

Briefly, rats (n = 15) were anesthetized with sodium thiopental (i.p.), placed on a stereotaxic frame (Stoelting, Wood Dale, IL, USA) and injected with 6-OHDA (n =10) or saline (controls, n = 5) unilaterally into two sites of the right medial forebrain bundle at the following coordinates (mm) relative to bregma and dural surface: (i) antero-posterior (AP) = −4.0, medio-lateral (ML) = −0.8, dorso-ventral (DV) = −8.0 tooth bar at +3.4 (9 μg/3 μL) and (ii) AP = −4.4, ML = −1.2, DV = −7.8 tooth bar at −2.4 (7.5 μg/3 μL). Animals were euthanized 8 weeks after 6-OHDA injection, brain and colon were dissected, and immediately frozen and processed for serial cryostatic sections (40 μm), or fixed in cold 4% neutral formalin, processed for paraffin-embedding and sectioning (5 μm). Immunohistochemical staining for tyrosine hydroxylase (TH) and total dopaminergic cell count were performed in brain cryostatic sections to assess striatal dopaminergic terminal damage and neuronal loss in the *substantia nigra pars compacta* (SNc) (Pellegrini et al., 2016b).

The absence of TH staining within the striatum, expressed as the percentage of striatal volume deprived of TH immunoreactivity, pointed out the occurrence of dopaminergic neurodegeneration following 6-OHDA injection. The total number of dopaminergic cells in SNc of both hemispheres was counted using stereological analysis (STEREO INVESTIGATOR software on a Neurolucida computer controlled microscopy system, Microbrightfield Inc., VT, USA) (Blandini et al., 2004). The cut-off level for the striatal lesion has been set at 98%, while for the lesion in the SNc at 95%.

2.2. Histology and histochemical detection of mucin and collagen deposition

Before use, colonic full-thickness sections were deparaffinized, rehydrated and processed for the staining of haematoxylin/eosin and histochemical toluidine blue in order to evaluate eosinophil density and quantify mucin, which appeared as purple/violet drops after metachromatic staining. Collagen was detected by Sirius Red/Fast Green (SR/FG) staining, which is able to label collagen and non-collagen proteins as red and green deposits, respectively (Segnani et al., 2015).

2.3. Immunoenzymatic histochemistry

Colonic sections were incubated overnight at 4 °C with the following primary antibodies (for reagents see Table 1): anti-claudin-1 (epithelial cells), anti-transmembrane 16A/Anoctamin 1 (TMEM16A/ANO1) [epithelium and interstitial cells of Cajal (ICCs)]. Sections were then exposed to appropriate biotinylated immunoglobulins, peroxidase-labelled streptavidin complex and 3.3′-diaminobenzidine tetrahydrochloride, counterstained and examined by a Leica DMRB light microscope equipped with a DFC480 digital camera (Leica Microsystems, Cambridge, UK).

2.4. Immunofluorescence

Double immunofluorescence studies were performed to detect cellular phenotypes and proliferating cells of the colonic wall, as previously described (Ippolito et al., 2015). In brief, sections were incubated with Protein Block Serum Free, primary antibodies [anti-S100, −α-SMA, −desmin, −vimentin, −proliferating cell nuclear antigen (PCNA)] diluted in phosphate-buffered saline (PBS) (overnight at 4 °C), appropriate fluorophore-conjugated secondary reagents, and finally with TO-PRO3 for nuclear counterstaining (for reagents see Table 1). Sections were examined under a Leica TCS SP8 confocal laser-scanning microscope (Leica Microsystems, Mannheim, Germany) and sample were scanned by means of 40× and 63× oil lens, using a sequential scan procedure.

2.5. Western blot analysis of claudin-1, TMEM/ANO1, collagen and vimentin expression

Colonic specimens were dissected, weighed and homogenized in lysis buffer containing: HEPES 10 mmol/L, NaCl 30 mmol/L, ethylenediaminetetraacetic acid 0.2 mmol/L, phenylmethylsulfonyl fluoride 2 mmol/L, leupeptin 10 μg/mL, aprotinin 10 μg/ml, sodium fluoride 1 mmol/L, sodium orthovanadate 1 mmol/L, glycerol 2%, $MgCl_2$ 0.3 mmol/L, and Triton-X 100 1%, using a polytron homogenizer. Homogenates were centrifugated at 15,000 *g* for 15 min at 4 °C, and then the supernatants were stored at −80 °C. Protein concentration was determined by the Bradford method (Protein Assay Kit; Bio-Rad, Hercules, CA). To perform western blot analysis of claudin-1, TMEM/ANO1, collagen and vimentin, equivalent amounts of protein lysates (50 μg) were separated by electrophoresis. The blots were then blocked

Table 1
Primary and secondary antibodies and reagents employed in the study.

Primary antibodies	Clone	Species	Dilution	Source
anti-TH	MAb	mouse	1:2000	Chemicon International, Temecula, CA, USA
anti-claudin-1	PAb	rabbit	1:500	Abcam, Cambridge, UK
anti-S100 antigen	PAb	rabbit	1:4000	DakoCytomation, Glostrup, Denmark
anti-transmembrane 16A/Anoctamin 1 (TMEM/ANO1)	PAb	goat	1:100	Santa Cruz Biotechnology, Inc., Heidelberg, Germany
anti-α-SMA	MAb	mouse	1:100	DakoCytomation, Glostrup, Denmark
anti-desmin	PAb	rabbit	1:500	Abcam, Cambridge, UK
anti-vimentin	MAb	rabbit	1:1000	Abcam, Cambridge, UK
anti-proliferating cell nuclear antigen (PCNA)	MAb	mouse	1:1000	Santa Cruz Biotechnology, Heidelberg, Germany
Secondary antibodies and reagents				
Biotinylated anti-mouse IgG (H + L) affinity purified		goat	1:200-1000	Vector Laboratories, Burlingame, CA, USA
Biotinylated anti-rabbit IgG (H + L) affinity purified		goat	1:200	Vector Laboratories, Burlingame, CA, USA
Biotinylated anti-goat IgG (H + L) affinity purified		rabbit	1:200	Vector Laboratories, Burlingame, CA, USA
Alexa Fluor^{R} 488 goat anti-mouse SFX kit - Highly cross-adsorbed		goat	1:300	Invitrogen, Eugene, Oregon, USA
Alexa Fluor™ 568 goat anti-rabbit IgG (H + L)		goat	1:300	Molecular Probes, Eugene, Oregon, USA
Streptavidin, Alexa Fluor^{R} 555 conjugated			1:300	Molecular Probes, Eugene, Oregon, USA
TO-PRO^{R}-3 iodide 642/661			1:10000	Molecular Probes, Eugene, Oregon, USA
Protein Block Serum Free			Ready to use	DakoCytomation, Glostrup, Denmark
Vectastain ABC kit			Ready to use	Vector Laboratories, Burlingame, CA, USA
3.3′-diaminobenzidine tetrahydrochloride			Ready to use	DakoCytomation, Glostrup, Denmark
Neutral buffered formaldehyde, ethanol, xylene, DPX mountant			Ready to use	Sigma-Aldrich & CO., St. Louis, MO, USA
Peroxidase-conjugated antibodies	PAb	goat	1:10000	(Santa Cruz Biotechnology, Santa Cruz, CA)

overnight with 5% non-fat dried milk in PBS and incubated overnight at room temperature with primary antibodies (see Table 1). After washings with 0.1% Tween-20 in Tris-buffered saline, horseradish peroxidase-conjugated secondary antibodies (see Table 1) were added for 1 h at room temperature. After washings with 0.1% Tween-20 in Tris-buffered saline, immunoreactive bands were visualized by incubation with chemiluminescent reagents and exposed to Kodak Image Station 440 for signal detection and densitometric image analysis. To ensure equal sample loading, blots were stripped and reprobed for β-actin determination by a specific primary antibody (see Table 1).

2.6. Image analysis and statistics

For histochemical and immunohistochemical staining, sections were examined by a Leica DMRB light microscope, equipped with a DFC480 digital camera (Leica Microsystems); for each group, representative photomicrographs were shot and analyzed quantitatively using the Image Analysis System 'L.A.S. software version 4.5' (Leica Microsystems, Cambridge, UK). Two blind investigators (C.I. and C.S.) carried out cell-counting independently and assessed the colorimetric threshold values to detect antigen expression levels. Cell densities were evaluated as cell number per analyzed areas (mm^2) for eosinophils, glial cells and ICCs. Toluidine blue-positive mucin, SR-positive fibres, and immunostaining expression were calculated as ratio between area of the stained fields and the total tissue area examined (percentage positive pixels [PPP]), as previously reported (Pellegrini et al., 2016b; Segnani et al., 2015). Data obtained from all the examined fields for each rat were averaged and used to calculate mean values ± SEM for each experimental group, which were plotted in graphs. Student's *t*-test (for unpaired data) was used to show statistical differences with $P \leq .05$.

3. Results

3.1. Immunohistochemical analysis of TH in brain

6-OHDA rats ($n = 10$) displayed a significant decrease in dopaminergic striatal terminals (98%) and dopaminergic neurons in SNc (95%) of the injected hemisphere (Fornai et al., 2016). No differences in TH immunoreactivity between hemispheres were detected in sham-operated rats (data not shown).

3.2. Histology

The gross morphology of colonic wall did not show relevant tissue alterations in 6-OHDA rats, as compared with controls: intact mucosal, submucosal and muscle layers were appreciated, apart from mucosal and submucosal leukocyte infiltration, with a significant increase in eosinophils, along with a considerable amount of submucosal vessels rich in leukocytes (Fig. 1).

3.3. Colonic epithelium and mucosal S100-positive cells

In control rats, lining epithelial cells expressed an abundant amount of claudin-1, which is one of the main components of tight junctions, and TMEM16A/ANO1, a transmembrane protein involved in epithelial barrier functions (Fig. 2). In 6-OHDA rats, the colonic epithelium displayed a significant decrease in claudin-1 and TMEM16A/ANO1 immunostaining (2.30 and 2.8 fold decrease vs controls, respectively). With regard for mucus producing cells, 6-OHDA rats displayed a significant increase in mucin expression (10.29 fold increase vs controls) with mucin drop-filled goblet cells localized at both the upper and lower regions of tubular glands. The density of S100-positive cells within the *lamina propria* was significantly increased in 6-OHDA rats (1.53 fold increase vs controls) (Fig. 2).

3.4. Histochemical detection of collagen fibres

The colon of 6-OHDA rats showed a transmural deposition of collagen fibres, as compared with controls. In particular, a significant deposition of red-stained collagen fibres was observed in the *tunica mucosa/submucosa* (2.06 fold increase vs controls) and *muscularis* (2.14 fold increase vs controls), mainly in the submucosal border, myenteric ridge and serosal layer (Fig. 3).

3.5. Cellular phenotypes and proliferation in the tunica mucosa and muscularis

An intense proliferative activity of the colonic epithelium was observed in 6-OHDA rats, as compared with controls. These changes were documented by high expression of PCNA-positive cells in the crypts of tubular glands (Fig. 4A). The *lamina propria* of 6-OHDA animals showed an increased density of vimentin-positive pericriptal cells, some of which displayed a proliferative, PCNA-positive phenotype (Fig. 4A).

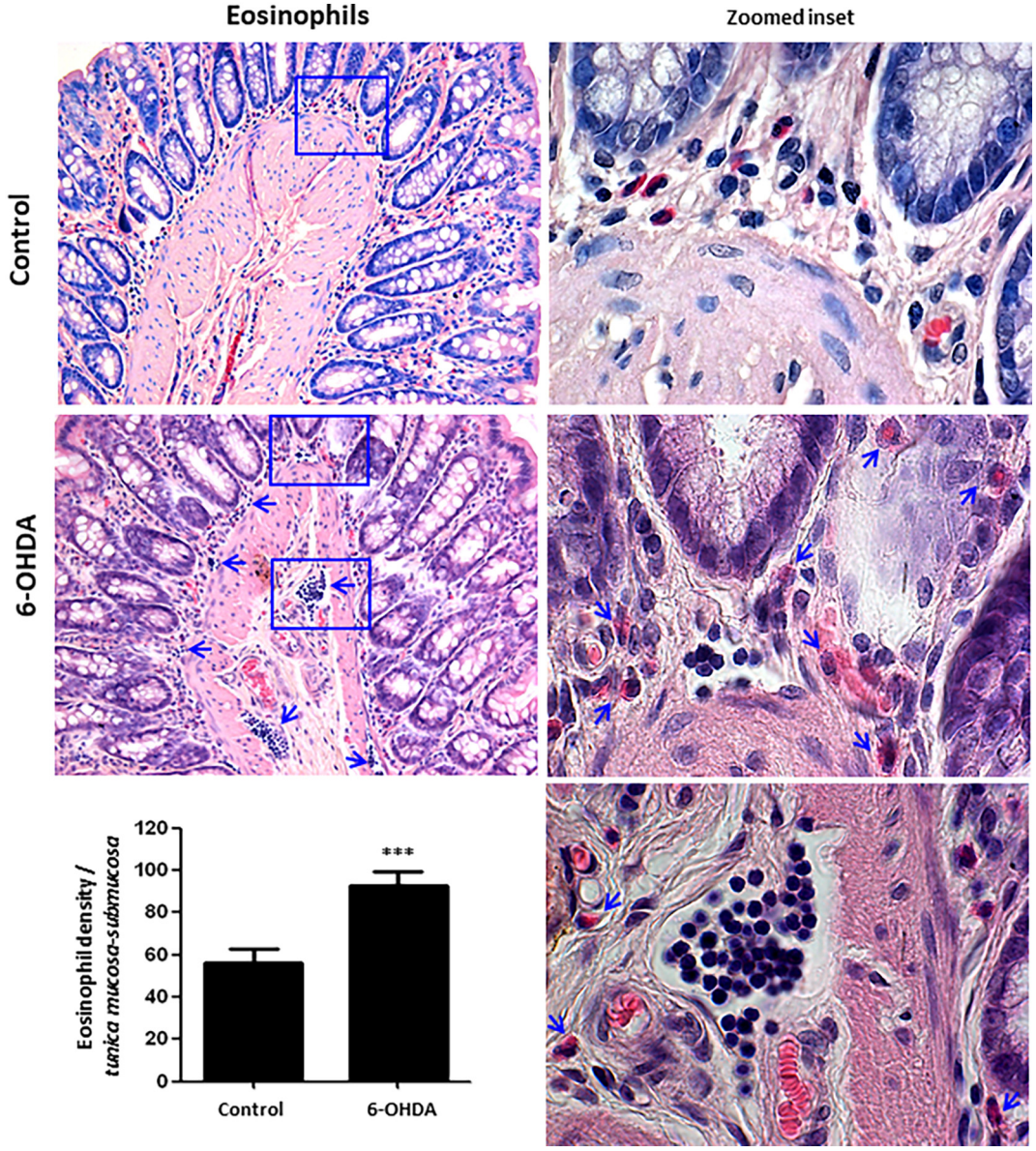

Fig. 1. Unchanged gross morphology of colon in 6-OHDA rats apart from leukocyte infiltration.
Representative pictures of haematoxylin/eosin-stained samples of full-thickness, cross-sectioned colon obtained from control or 6-OHDA animals, showing mucosal and submucosal vessels full of leukocytes (arrows) and leukocyte infiltration rich in eosinophils (arrows in insets). Original magnification 20× (haematoxylin/eosin; zoomed inset 100×). Column graphs display the mean values of eosinophil density calculated as ratio of cell number over the respective tissue area examined ± SEM. Student's test; ***$P \leq .001$.

The appreciable amount of α-SMA and desmin observed in the smooth muscle cells of *tunica muscularis* under control conditions was decreased in 6-OHDA animals (Fig. 4B). Colonic tissues from 6-OHDA rats showed also an increased number of vimentin-positive elongated cells, many of which were co-stained with α-SMA. The latter were found mainly among the smooth muscle cells of *tunica muscularis* and in the myenteric ganglia, as compared to controls (Fig. 4B). In 6-OHDA rats, an appreciable nuclear reactivity for PCNA was found in several smooth muscle cells as well as in muscle and ganglionic vimentin-positive cells (Fig. 4B).

3.6. Colonic ICCs

In control colon, ICCs were clearly detected by TMEM16A/ANO1 immunostaining as round-shaped cells endowed with elongated processes and lined up along the submucosal and myenteric ridges, enveloping the myenteric ganglia and forming appreciable interganglionic networks, as well as scattered cells throughout the muscle layers. In 6-OHDA rats, the density of myenteric ICCs was decreased significantly (1.57 fold decrease vs controls) (Fig. 5). In the circular muscle layer of 6-OHDA rats, the ICC density remained unchanged, but their cellular extensions and TMEM16A/ANO1 immunoreactivity were significantly decreased (2.18 fold decrease vs controls) (Fig. 5).

3.7. Expression of claudin-1, TMEM/ANO1, collagen and vimentin

Western blot analysis revealed the constitutive expression of claudin-1 and TMEM/ANO/1 in colonic tissues from control rats (Fig. 6B and C). In colonic tissues from 6-OHDA rats, a significant decrease in the expression of these proteins was detected (Fig. 6A and B).

With regard for collagen and vimentin, 6-OHDA animals displayed a significant increase in the colonic expression of these proteins, as compared with controls (Fig. 6A and D).

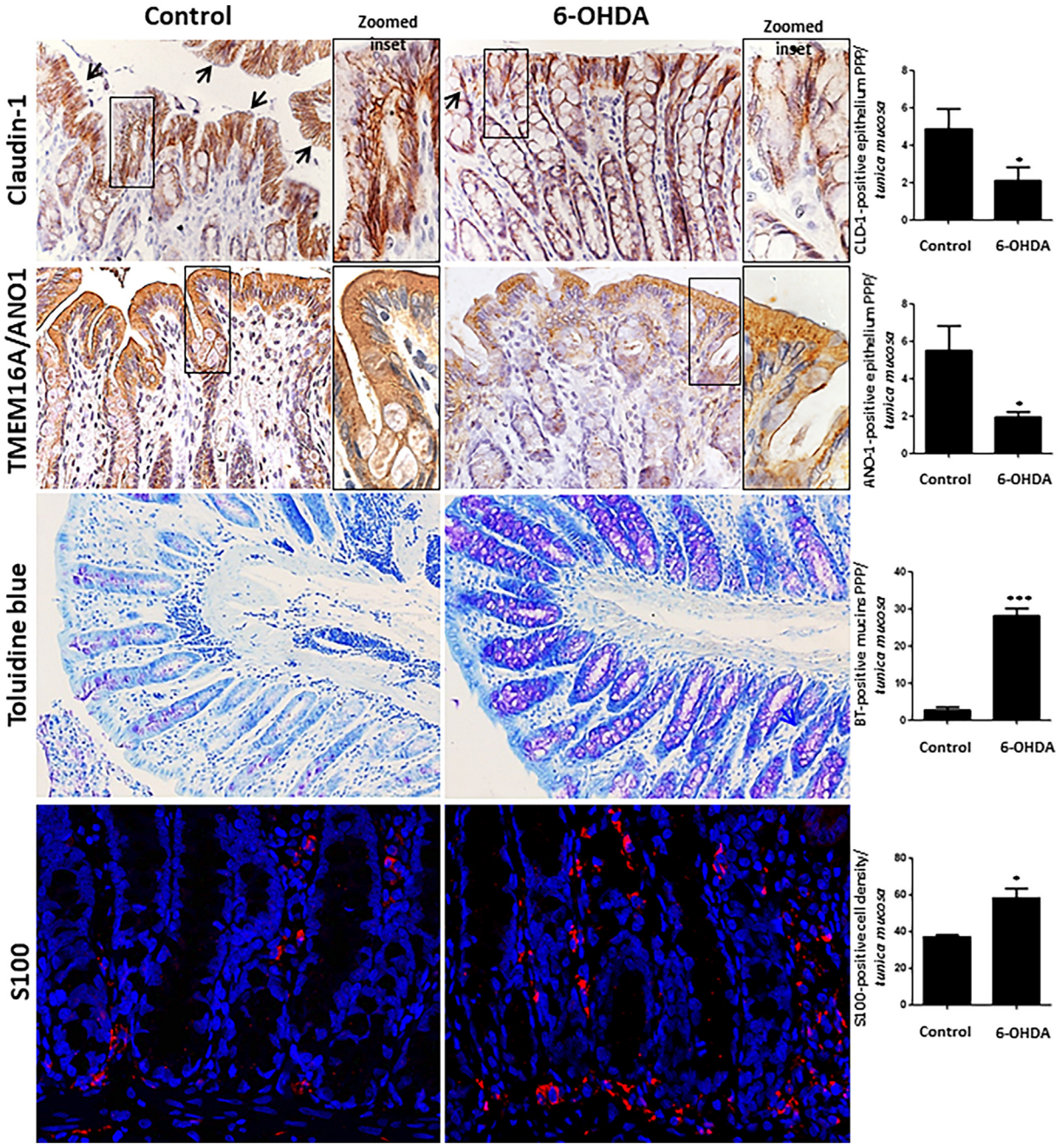

Fig. 2. Changes in colonic mucosal barrier with decreased expression of claudin-1, impairment of epithelium and mucus, and increased glial cells in 6-OHDA rats. Representative photomicrographs of claudin-1, TMEM16A/ANO-1 and S100 immunostaining, together with toluidine blue histochemistry of full-thickness, cross-sectioned colon obtained from control and 6-OHDA rats. Original magnification 20×, 40×; zoomed insets 100×. Column graphs display the mean values of percentage of positive pixels (PPP) and S100-positive cell density within the respective tissue area examined ± SEM. Student's test; * $P \leq .05$, *** $P \leq .001$. (For interpretation of the references to colour in this figure legend, the reader is referred to the web version of this article.)

4. Discussion

Previously, we observed that the induction of central dopaminergic denervation elicited bowel motor dysfunctions and enteric inflammation (Fornai et al., 2016; Pellegrini et al., 2016b). In this context, the presence of a chronic low-grade enteric inflammation might promote severe pathological alterations of gut wall, which, in turn, could contribute further to functional alterations (Speca et al., 2012). On these bases, the present study examined a series of morphological features in the colon of rats following 6-OHDA-induced central dopaminergic denervation.

As a first step, we evaluated the presence of colonic inflammation after 8 weeks from denervation. Our results showed that nigrostriatal denervation elicits the occurrence of colonic inflammation, characterized by interstitial leukocyte infiltration rich in eosinophils and vessels stuffed with leukocytes within the *tunica mucosa* and *submucosa*. These findings corroborate previous evidence in both animal models and patients showing that central nigrostriatal neurodegeneration is associated with enteric inflammation (Devos et al., 2013; Pellegrini et al., 2016b).

The presence of enteric inflammation, besides contributing to bowel motor dysfunctions, can impair also the intestinal mucosal barrier with consequent alterations of intestinal permeability and secretory functions (Lechuga and Ivanov, 2017; Michielan and D'Inca, 2015). Based

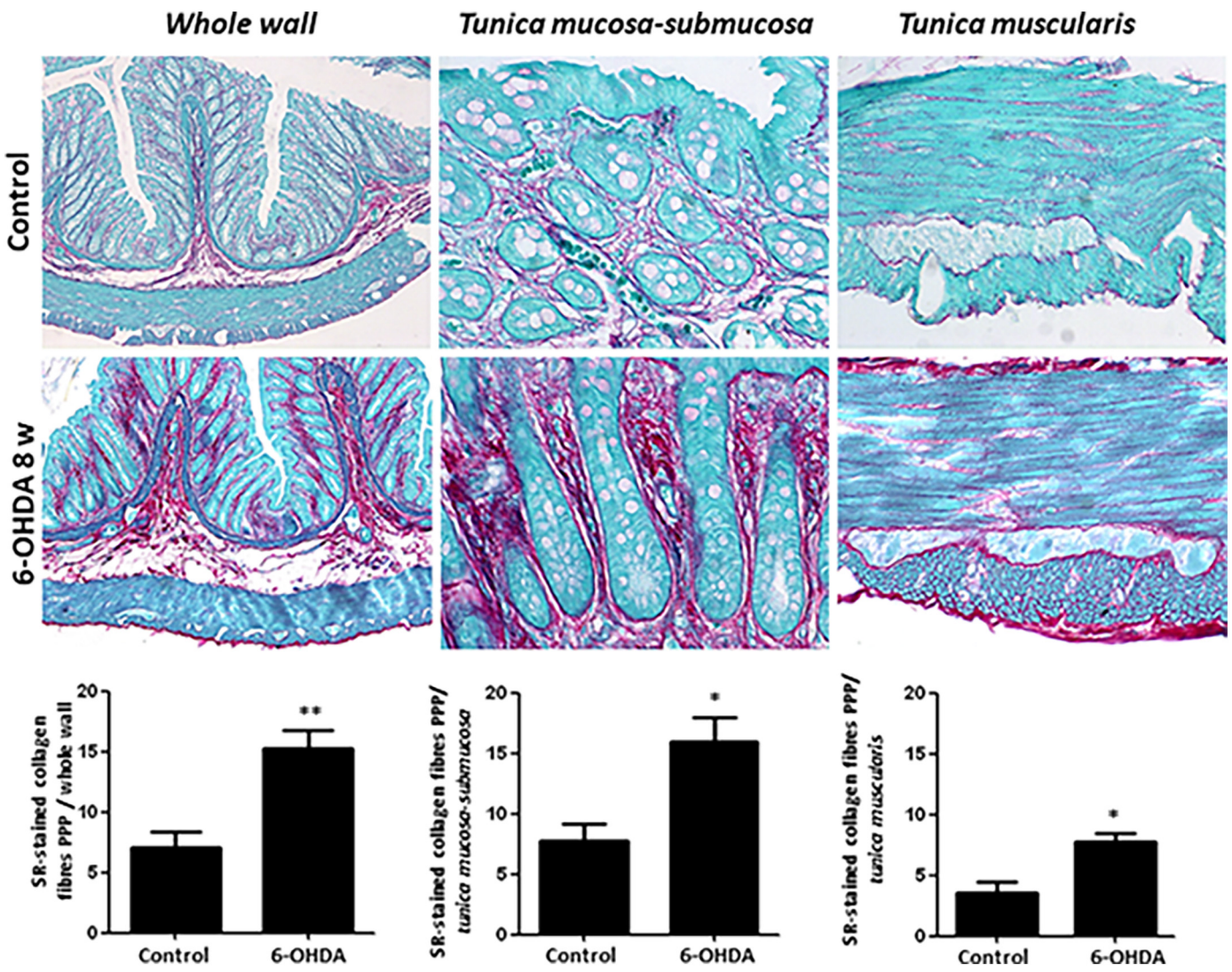

Fig. 3. Increased collagen fibres in the colon from 6-OHDA rats.
Representative photomicrographs of Sirius red (*SR*)-stained collagen fibres and fast green (FG)-stained non-collagen proteins in samples of full-thickness, cross-sectioned colon obtained from control or 6-OHDA animals. Red-stained collagen fibres were quantified in the whole colonic wall and, separately, in the *tunica mucosa/submucosa* and *muscularis*. Original magnification 10× (whole wall) and 40× (*tunica mucosa* and neuromuscular compartment). Column graphs display the mean values of percentage of positive pixels (PPP) of red-stained collagen fibres within the respective tissue area examined ± SEM. Statistics: Student's test; *P ≤ .05, **$P \leq .01$. (For interpretation of the references to colour in this figure legend, the reader is referred to the web version of this article.)

on these considerations, in the second part of the study we examined the morphological features of intestinal mucosal barrier. In particular, we paid attention to the tight junction protein claudin-1 and mucin, both regarded as pivotal factors involved in the maintenance of barrier integrity (Dupont et al., 2014; Groschwitz and Hogan, 2009). Indeed, claudin-1 is regarded as one of the main structural determinants of tight junctions pivotally involved in building molecular networks of intramembranous strands, which seal together tightly adjacent cells (Lu et al., 2013). Our findings highlighted a decreased expression of claudin-1 in 6-OHDA rats, thus providing the demonstration that nigrostriatal degeneration is followed by impairments of intestinal epithelial barrier, which could lead to an increased intestinal permeability. These changes would facilitate the translocation of microbial flora into the mucosa, with consequent chronicization of the inflammatory response and further worsening of bowel dysfunctions (Rescigno, 2011). In line with this view, clinical studies have documented morphological alterations of the intestinal barrier, with alterations of occludin and zonulin-1 distribution and expression in colonic biopsies from PD patients (Balda and Matter, 2009; Clairembault et al., 2015; Perez-Pardo et al., 2019).

When considering mucin expression, we detected an increase in the colonic epithelial cells of 6-OHDA rats. Mucin released by goblet cells contributes to the formation of a thick, hydrated mucus layer, subjected to renewal every 1–2 h, to prevent an excessive direct contact of invasive pathogens with the epithelial cell surface (Dupont et al., 2014; Pelaseyed et al., 2014). In our hands, 6-OHDA animals developed a mucous metaplasia of colonic epithelium with an increased number of goblet cells, which were full of metachromatic, acid mucin contents. The overexpression of mucins and mucous metaplasia occurred in concomitance with a fast epithelial turnover in colonic crypts. This enhanced proliferative activity might reflect a stress condition, forcing these cells to a fast renewal and differentiation into goblet phenotype to strengthen the intestinal barrier. In this light, the increase in mucin expression could be viewed as a compensatory response to the alterations of epithelial barrier (claudin-1 deficiency) and enteric inflammation. Consistent with these results, recent studies reported an increase in mucin expression in colonic specimens from patients with Crohn's disease (Dorofeyev et al., 2013).

The production of mucus from goblet cells is controlled by a number of factors, among which TMEM16A/ANO1 (Johansson and Hansson,

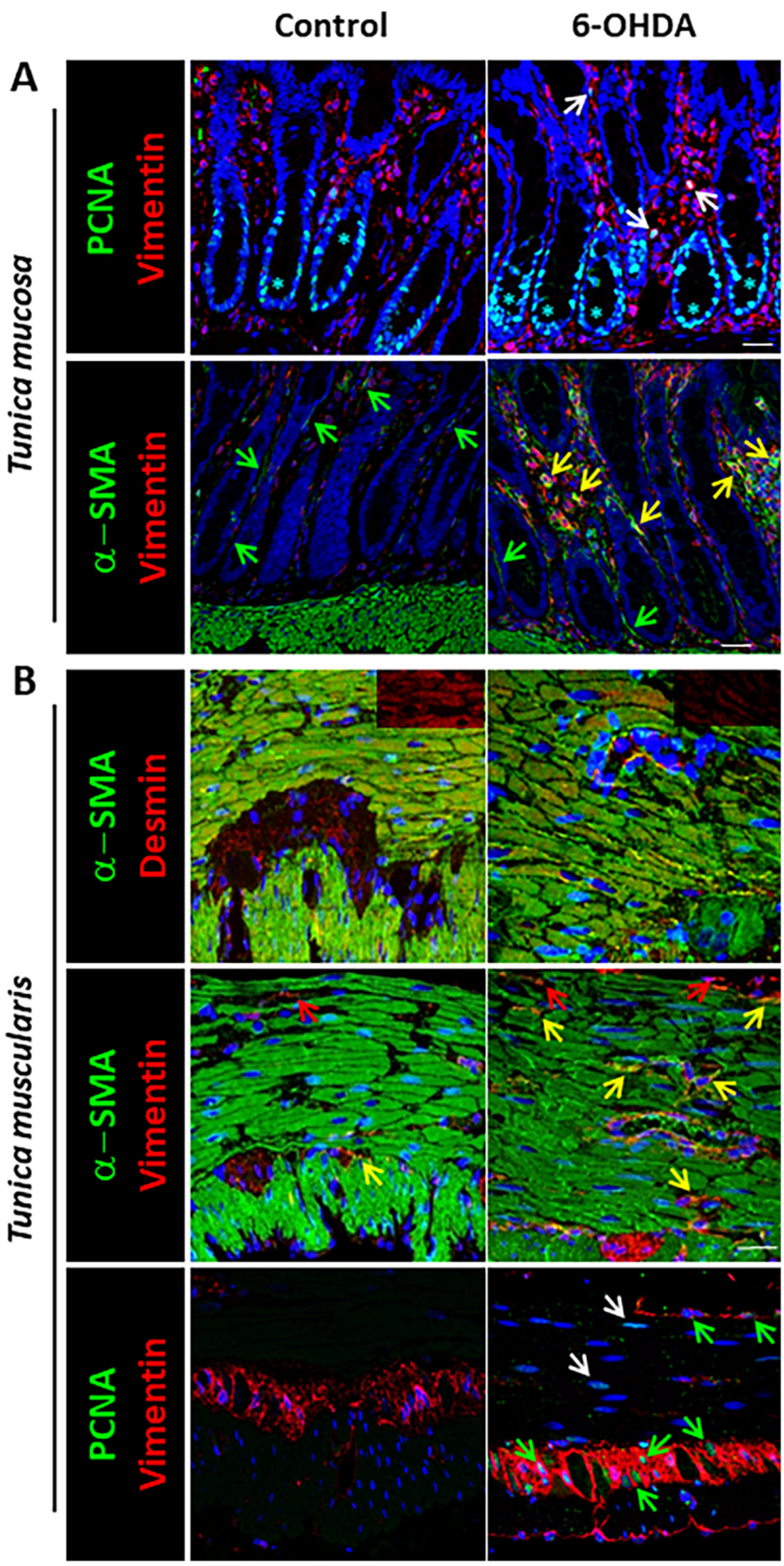

Fig. 4. Double immunofluorescence staining of colonic mucosal layer (A) and neuromuscular compartment (B) in 6-OHDA rats.

(A) Increased density of proliferating cells in epithelial crypts and vimentin-positive cells in the lamina propria. Representative images of PCNA (green)/vimentin (red) or α–SMA (green)/vimentin (red) double immunostaining of the colonic mucosal layer. 6-OHDA rats displayed increased PCNA-positive nuclei (cyan; astericks) in epithelial cells of the tubular crypts and vimentin-positive cells in the *lamina propria* (cyan; white arrows). α–SMA-positive cells (green arrows), abundantly present in the *lamina propria* of controls, were reduced in 6-OHDA rats, which displayed an increase in vimentin-positive cells (red cells) and several cells with a yellowish fluorescence (colocalization of α–SMA and vimentin; yellow arrows). Nuclear counterstaining with TO-PRO3. Original magnification 400× oil lens.

(B) Increased expression of vimentin-positive cells in the tunica muscularis. Representative images of α–SMA (green)/desmin (red) or α–SMA(green)/vimentin (red) and PCNA (green)/vimentin (red) double immunofluorescence staining of colonic muscle layers. In 6-OHDA rats, the *tunica muscularis* showed a decrease in both α–SMA (green) and desmin (highlighted in the red single channel; insets) expression. 6-OHDA animals displayed an increased number of vimentin-positive cells (red arrows), many of which presented a co-localization with α–SMA (yellow arrows). Myenteric ganglia were intensely vimentin-immunostained and displayed several PCNA-positive nuclei (green arrows), which were also found in the *tunica muscularis* within vimentin-negative (white arrows) and vimentin-positive (green arrows) cells. Nuclear counterstaining with TO-PRO3. Original magnification 63× oil lens. (For interpretation of the references to colour in this figure legend, the reader is referred to the web version of this article.)

2013; Pedemonte and Galietta, 2014). This protein takes part to several functions in epithelial barriers by hydrating actively the mucosal surfaces (Keely et al., 2012), maintaining mucins well hydrated and fluid, and facilitating mucin release from goblet cells (Pedemonte and Galietta, 2014). In our study, the colon of 6-OHDA rats displayed a reduced expression of TMEM16A/ANO1 along with an upregulation of mucin in epithelial cells. In this context, the lack of TMEM16A/ANO1 might compromise the chemico-physical properties and secretion of

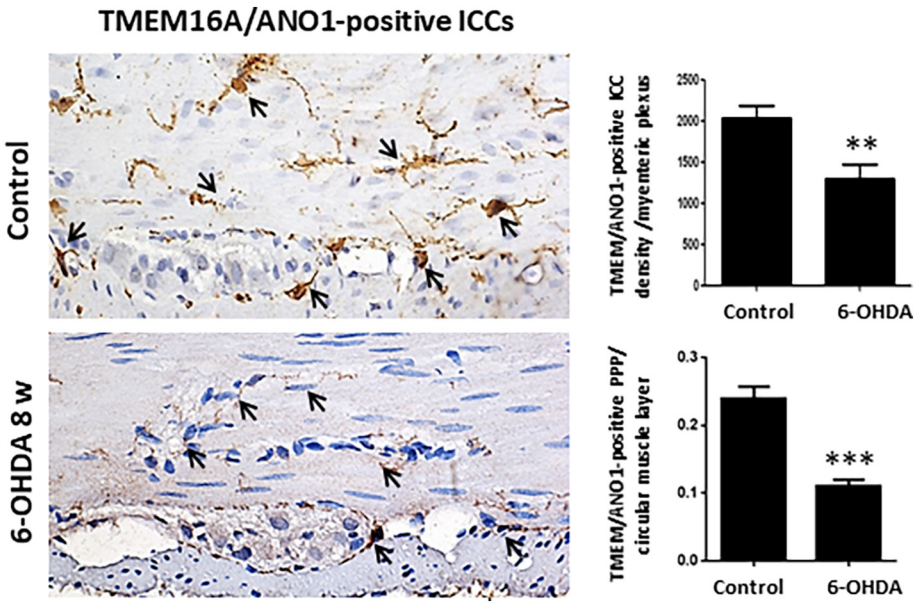

Fig. 5. Downregulation of interstitial cells of Cajal (ICCs) in 6-OHDA rats.
Representative photomicrographs of TMEM16A/ANO-1 immunostaining of ICCs lining the myenteric ridge in full-thickness cross-sectioned colon. Original magnification 40×. Column graphs display the mean values of TMEM16A/ANO-1-positive cell density within the respective tissue area examined ± SEM, and percentage of positive pixels (PPP) of brown-stained ICCs calculated on the tissue area examined ± SEM. Statistics: Student's *t*-test; **P ≤ .01, *** P ≤ .001. (For interpretation of the references to colour in this figure legend, the reader is referred to the web version of this article.)

mucus as well as the active mucosal hydration, thus impairing the primary mechanisms of innate epithelial defense against pathogens. Furthermore, an impaired chloride secretion could decrease the fecal water content with a consequent delay in colonic transit and possible occurrence of constipation. Supporting this hypothesis, Zhang et al., 2015 showed that stool water content was reduced in 6-OHDA rats (Zhang et al., 2015). On the other hand, it cannot be excluded that the decreased stool hydration could arise from an enhanced water reabsorption consequent to a delayed colonic transit. Whatever the predominant mechanism, it is conceivable that the enteric inflammation following nigrostriatal denervation might compromise the intestinal mucosal barrier, with consequent alterations of permeability and mucus production, contributing further to bowel motor dysfunctions. Clearly, this remains an open issue awaiting clarifications by future investigations.

A population of S100-positive cells, referred as mucosal glia and contributing to the maintenance of the integrity of intestinal barrier, has been identified just beneath the gut lining epithelium (Kabouridis et al., 2015; Neunlist et al., 2013). Of note, alterations in the expression of GFAP and S100-β glial markers have been described in several gastrointestinal disorders characterized by barrier dysfunctions (Brun et al., 2017; Cirillo et al., 2011; Gulbransen and Sharkey, 2012). Based on this knowledge, we examined the patterns of subepithelial glial cells in colonic tissues from 6-OHDA animals. The experiments revealed a significant increase in S-100-positive cells in the tunica mucosa, indicating that nigrostriatal neurodegeneration leads to an increased presence of glial cells in this colonic districts. Such results are consistent with a previous study displaying enteric glial activation in colonic tissues from PD patients (Devos et al., 2013). However, these authors observed an increased expression of GFAP and Sox-10, but not S100-β (Devos et al., 2013). This discrepancy could depend on the different experimental approaches, as they assessed quantitatively mRNA expression in the overall tissue specimens captured by biopsy, while we carried out a specific immunohistochemical analysis of the mucosal and submucosal layers. The upregulation of S-100-positive sub-epithelial glial cells, as observed in 6-OHDA rats, might be interpreted as an attempt of counteracting the impairment of claudin-1 and the proliferative trend of colonic epithelium, which are both known to be under the control of mucosal glia (Neunlist et al., 2007). In this regard, further focused studies aimed at characterizing the role played by intramucosal enteric glia in the maintenance of the integrity of epithelial barrier should be performed.

Several studies have shown that enteric inflammation could promote abnormal tissue repair with consequent development of fibrosis (Ippolito et al., 2015; Rieder et al., 2007). For these reasons, and taking also into account previous findings in bowel specimens from PD patients (Devos et al., 2013), we investigated the presence of fibrotic processes in colonic tissues from 6-OHDA rats. Our results highlighted a remarkable collagen deposition throughout the whole thickness of colon, thus providing original evidence that, following nigrostriatal denervation, the colon undergoes a fibrotic wall remodelling. Such colonic fibrosis was further corroborated by an increase in vimentin-positive fibroblast/myofibroblast-like cells in the mucosal and submucosal layers, some of which with α–SMA-positive cytoplasm and PCNA-positive nuclei, a typical feature of an activated cellular phenotype. Of note, our findings are consistent with several clinical observations, displaying the switch of intestinal mesenchymal cells towards a fibroblast/myofibroblast cell phenotype in the presence of chronic and persistent inflammation (Ippolito et al., 2016; Ippolito et al., 2015; Speca et al., 2012).

As anticipated above, at level of the *tunica muscularis*, 6-OHDA rats displayed an increase in vimentin-positive cells with scattered PCNA-stained nuclei, along with a decreased muscle phenotype, stigmatized by a downregulation of desmin and α–SMA contents. Likewise, myenteric ganglia were found to be intensely vimentin-positive and showed PCNA-positive nuclei. These results show a cell phenotype modulation in the colonic *tunica muscularis* following central dopaminergic denervation. In particular, the quiescent, non-proliferative [PCNA-negative] smooth muscle cell phenotype [α-SMA-positive/desmin-positive/vimentin-negative] was replaced by deranged smooth muscle cells with reduced α-SMA and desmin immunoreactivity, some of which with PCNA-positive nuclei. Furthermore, 6-OHDA rats displayed several fibroblast-like cells [vimentin-positive], some of which showed a proliferative phenotype [PCNA-positive] and co-expressed α-SMA-positivity, a hallmark of myofibroblasts (Marlow and Blennerhassett, 2006).

In keeping with previous studies on enteric muscle layers in experimental colitis (Ippolito et al., 2016; Ippolito et al., 2015; Nair et al., 2011), the fibrogenic remodelling, detected in the colon of 6-OHDA animals, provides pioneering evidence that central dopaminergic denervation leads to a cellular fibrotic switch in the *tunica muscularis*. Taken together, these results point out that the occurrence of chronic low-grade colonic inflammation upon nigrostriatal denervation promotes a full-thickness structural remodelling, characterized by diffuse fibrotic deposition in the colonic wall, which might contribute to bowel

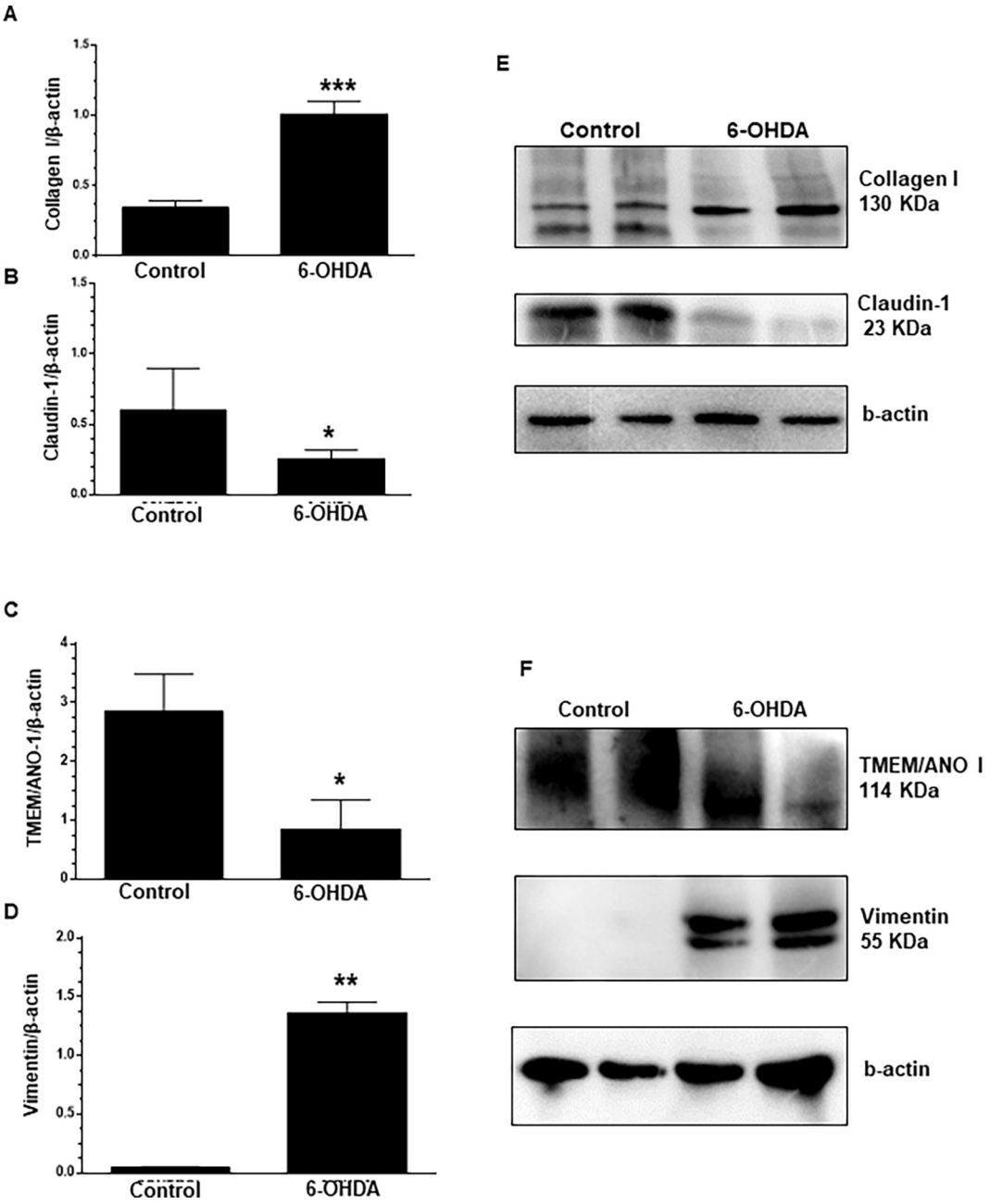

Fig. 6. Protein expression of collagen, claudin-1, TMEM/ANO1 and vimentin in 6-OHDA rats.
Western blot analysis of collagen (A), claudin-1 (B), TMEM/ANO-1 (C) and vimentin (D) in the colon obtained from control and 6-OHDA rats. Each column represents the mean ± SEM obtained from 8 animals. Student's t-test; *P ≤ .05, **P ≤ .01, ***P ≤ .001.

motor dysfunctions.

Previous studies have documented that a chronic low-grade inflammation in the gut can alter digestive motility, through alterations of enteric nerve pathways, ICCs or smooth muscle cells, suggesting a relationship between enteric inflammation and modifications of enteric motor activity (Khan and Collins, 2006). In particular, ICCs are regarded as main players in the regulation of motor functions in the gut wall, ensuring a coordinated muscular activity (Furness, 2012). In the setting of bowel inflammation, this neuromuscular network undergoes remarkable alterations, which lead to gut dysmotility (De Giorgio et al., 2007). Based on this background, and considering also previous observations made both in PD patients and animal models (Cersosimo et al., 2013; Fornai et al., 2016; Pellegrini et al., 2016a; Pellegrini et al., 2016b), we examined the expression of ICCs in the colonic neuromuscular compartment of 6-OHDA animals (Huang et al., 2009). Our results revealed a significant reduction of the density of ICCs of the myenteric ridge along with a remodelling of circular ICCs with a loss of their extensions. To the best of our knowledge, these data provide an original demonstration of quantitative variations of colonic ICCs in a model of nigrostriatal dopaminergic neurodegeneration. Moreover, these observations are in live with previous studies showing a decreased density of ICCs in the colon from rats with colitis (Ippolito et al., 2015). Thus, the remodelling of ICCs, in terms of density and morphology, could contribute to the development of colonic dysmotility observed in animals with central dopaminergic neurodegeneration. However, whether ICC abnormalities in 6-OHDA rats depend on direct effects of inflammation [14, 17, 18], alterations reflecting primary glial damage [19] or fibrotic processes, require confirmation by further focused studies.

5. Conclusions

The present results point out that central nigrostriatal neurodegeneration is characterized by: 1) enteric inflammatory condition; 2) impairments of intestinal mucosal barrier; 3) remodelling of full-thickness colonic wall towards a fibrotic phenotype; 4) quantitative variations of ICCs. These results set a morphological basis for understanding functional bowel abnormalities associated with PD.

Author contributions

Carolina Pellegrini, Matteo Fornai and Luca Antonioli designed the study and wrote the manuscript. Chiara Ippolito, Cristina Segnani, Silvia Cerri, Mariella Errede and Francesca Garelli, Anna Nericcio performed experiments and prepared the figures. Daniela Virgintino, Rocchina Colucci, Corrado Blandizzi, Amelio Dolfi, Fabio Blandini and Nunzia Bernardini revised the manuscript.

Declaration of Competing Interest

The authors have no conflicts of interest to declare.

Acknowledgments

This research was supported by a grant from the Italian Ministry of Education, University and Research (PRIN 2009, project no. 2009MFSXNZ).

References

Balda, M.S., Matter, K., 2009. Tight junctions and the regulation of gene expression. Biochim. Biophys. Acta 1788, 761–767.
Bischoff, S.C., et al., 2014. Intestinal permeability–a new target for disease prevention and therapy. BMC Gastroenterol. 14, 189.
Blandini, F., et al., 2004. Neuroprotective effect of rasagiline in a rodent model of Parkinson's disease. Exp. Neurol. 187, 455–459.
Brun, P., et al., 2017. Saccharomyces boulardii CNCM I-745 supplementation reduces gastrointestinal dysfunction in an animal model of IBS. PLoS One 12, e0181863.
Cersosimo, M.G., et al., 2013. Gastrointestinal manifestations in Parkinson's disease: prevalence and occurrence before motor symptoms. J. Neurol. 260, 1332–1338.
Cirillo, C., et al., 2011. S100B protein in the gut: the evidence for enteroglial-sustained intestinal inflammation. World J. Gastroenterol. 17, 1261–1266.
Clairembault, T., et al., 2015. Structural alterations of the intestinal epithelial barrier in Parkinson's disease. Acta Neuropathol. Commun. 3, 12.
De Giorgio, R., et al., 2007. Novel therapeutic targets for enteric nervous system disorders. Trends Pharmacol. Sci. 28, 473–481.
Devos, D., et al., 2013. Colonic inflammation in Parkinson's disease. Neurobiol. Dis. 50, 42–48.
Dorofeyev, A.E., et al., 2013. Mucosal barrier in ulcerative colitis and Crohn's disease. Gastroenterol. Res. Pract. 2013, 431231.
Dupont, A., et al., 2014. Antimicrobial peptides and the enteric mucus layer act in concert to protect the intestinal mucosa. Gut Microbes 5, 761–765.
Fornai, M., et al., 2016. Enteric dysfunctions in experimental Parkinson's disease: alterations of excitatory cholinergic neurotransmission regulating colonic motility in rats. J. Pharmacol. Exp. Ther. 356, 434–444.
Furness, J.B., 2012. The enteric nervous system and neurogastroenterology. Nat. Rev. Gastroenterol. Hepatol. 9, 286–294.
Gordon, I.O., et al., 2014. Fibrosis in ulcerative colitis: mechanisms, features, and consequences of a neglected problem. Inflamm. Bowel Dis. 20, 2198–2206.
Groschwitz, K.R., Hogan, S.P., 2009. Intestinal barrier function: molecular regulation and disease pathogenesis. J. Allergy Clin. Immunol. 124, 3–20 (quiz 21-2).
Gulbransen, B.D., Sharkey, K.A., 2012. Novel functional roles for enteric glia in the gastrointestinal tract. Nat. Rev. Gastroenterol. Hepatol. 9, 625–632.
Huang, F., et al., 2009. Studies on expression and function of the TMEM16A calcium-activated chloride channel. Proc. Natl. Acad. Sci. U. S. A. 106, 21413–21418.
Ippolito, C., et al., 2015. An integrated assessment of histopathological changes of the enteric neuromuscular compartment in experimental colitis. J. Cell. Mol. Med. 19, 485–500.
Ippolito, C., et al., 2016. Fibrotic and vascular remodelling of colonic wall in patients with active ulcerative colitis. J. Crohns. Colitis. 10, 1194–1204.
Johansson, M.E., Hansson, G.C., 2013. Mucus and the goblet cell. Dig. Dis. 31, 305–309.
Kabouridis, P.S., et al., 2015. Microbiota controls the homeostasis of glial cells in the gut lamina propria. Neuron. 85, 289–295.
Keely, S., et al., 2012. Activated fluid transport regulates bacterial-epithelial interactions and significantly shifts the murine colonic microbiome. Gut Microbes 3, 250–260.
Khan, W.I., Collins, S.M., 2006. Gut motor function: immunological control in enteric infection and inflammation. Clin. Exp. Immunol. 143, 389–397.
Lechuga, S., Ivanov, A.I., 2017. Disruption of the epithelial barrier during intestinal inflammation: quest for new molecules and mechanisms. Biochim. Biophys. Acta, Mol. Cell Res. 1864, 1183–1194.
Lu, Z., et al., 2013. Claudins in intestines: distribution and functional significance in health and diseases. Tissue Barriers. 1, e24978.
Marlow, S.L., Blennerhassett, M.G., 2006. Deficient innervation characterizes intestinal strictures in a rat model of colitis. Exp. Mol. Pathol. 80, 54–66.
Michielan, A., D'Inca, R., 2015. Intestinal permeability in inflammatory bowel disease: pathogenesis, clinical evaluation, and therapy of leaky gut. Mediat. Inflamm. 2015, 628157.
Nair, D.G., et al., 2011. Proliferation modulates intestinal smooth muscle phenotype in vitro and in colitis in vivo. Am. J. Physiol. Gastrointest. Liver Physiol. 300, G903–G913.
Neunlist, M., et al., 2007. Enteric glia inhibit intestinal epithelial cell proliferation partly through a TGF-beta1-dependent pathway. Am. J. Physiol. Gastrointest. Liver Physiol. 292, G231–G241.
Neunlist, M., et al., 2013. The digestive neuronal-glial-epithelial unit: a new actor in gut health and disease. Nat. Rev. Gastroenterol. Hepatol. 10, 90–100.
Pedemonte, N., Galietta, L.J., 2014. Structure and function of TMEM16 proteins (anoctamins). Physiol. Rev. 94, 419–459.
Pelaseyed, T., et al., 2014. The mucus and mucins of the goblet cells and enterocytes provide the first defense line of the gastrointestinal tract and interact with the immune system. Immunol. Rev. 260, 8–20.
Pellegrini, C., et al., 2015. Gastric motor dysfunctions in Parkinson's disease: current preclinical evidence. Parkinsonism Relat. Disord. 21, 1407–1414.
Pellegrini, C., et al., 2016a. Intestinal dysfunction in Parkinson's disease: lessons learned from translational studies and experimental models. Neurogastroenterol. Motil. 28, 1781–1791.
Pellegrini, C., et al., 2016b. Alteration of colonic excitatory tachykininergic motility and enteric inflammation following dopaminergic nigrostriatal neurodegeneration. J. Neuroinflammation 13, 146.
Pellegrini, C., et al., 2018. Interplay among gut microbiota, intestinal mucosal barrier and enteric neuro-immune system: a common path to neurodegenerative diseases? Acta Neuropathol. 136, 345–361.
Perez-Pardo, P., et al., 2019. Role of TLR4 in the gut-brain axis in Parkinson's disease: a translational study from men to mice. Gut. 68, 829–843.
Rescigno, M., 2011. The intestinal epithelial barrier in the control of homeostasis and immunity. Trends Immunol. 32, 256–264.
Rieder, F., et al., 2007. Wound healing and fibrosis in intestinal disease. Gut. 56, 130–139.
Rota, L., et al., 2019. Constipation, deficit in colon contractions and alpha-synuclein inclusions within the colon precede motor abnormalities and neurodegeneration in the central nervous system in a mouse model of alpha-synucleinopathy. Transl. Neurodegener. 8, 5.
Segnani, C., et al., 2015. Histochemical detection of collagen Fibers by Sirius red/fast green is more sensitive than van Gieson or Sirius red alone in Normal and inflamed rat Colon. PLoS One 10, e0144630.
Speca, S., et al., 2012. Cellular and molecular mechanisms of intestinal fibrosis. World J. Gastroenterol. 18, 3635–3661.
Zhang, X., et al., 2015. Alteration of enteric monoamines with monoamine receptors and colonic dysmotility in 6-hydroxydopamine-induced Parkinson's disease rats. Transl. Res. 166, 152–162.